

Supplemental Information to

Computing Osmotic Permeabilities of Aquaporins AQP4, AQP5, and GlpF

from Near-Equilibrium Simulations

Thierry O Wambo¹, Roberto A Rodriguez¹ and Liao Y Chen^{1*}

¹Department of Physics, University of Texas at San Antonio, San Antonio, Texas 78249 U.S.A.

In Figs. S1 and S2, we illustrate the all-atom model systems of AQP4 and AQP5.

In Figs. S3 to S5, we show the relevant data and plot the osmotic currents of water through GlpF, AQP4, and AQP5 at 5°C and 25°C in response to a sub M osmolyte concentration gradient across the membrane. Linear regressions in all six cases give, with high confidence of fitting, results of single-channel permeabilities which are tabulated in Table I along with relevant data from the literature. Note that Fig. S3 is shown in the main text as Fig. 2.

In Fig. S6 to S8, we show mean square displacements of the waters inside the single-file region of GlpF, AQP4, and AQP5 at 5°C and 25°C respectively. Note that Fig. S6 is shown in the main text as Fig. 3. The slope of the curve divided by 2 gives the diffusion constant in the single file region from which the single channel permeability is obtained by multiplying it with the volume of a water molecule.

In Fig. S9, we show the free-energy profile of water permeation through AQP4, which was computed from the single-file water density $n(z)$ inside the water channel as a function of the z -coordinate,

$$G(z) - G(z_0) = -k_B T \ln(n(z)/n(z_0))$$

where z_0 is the reference point that can be chosen arbitrarily. The barrier in this Gibbs free energy profile (the maximum minus the minimum) is not equal to the Arrhenius activation barrier because it contains the entropic contribution $T(S(z)-S(z_0))$ in proportion to the absolute temperature T .

In Figs. S10 to S12, we illustrate the AQP4 and 5 channels. Noting how the ar/R residues (Arg and His shown in large spheres) are anchored by the surrounding residues, we can see why the fluctuations are very small in AQP4 and the channel remain open all the time for water conduction. The fluctuations of the ar/R residues are much easier in AQP5 and the channel switches automatically between open and closed for water transport.

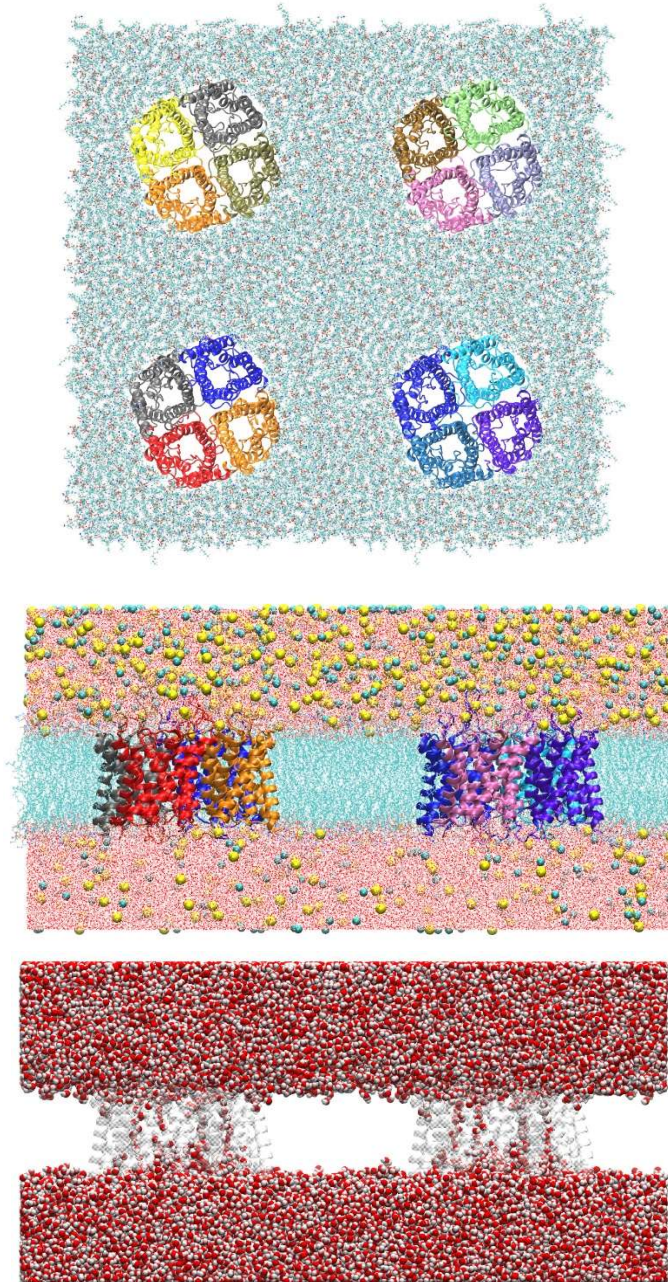


Fig. S1. Model system of AQP4 at 25°C. Shown in the top panel are the top view of four AQP4 tetramers (16 individual water channels/monomers) embedded in a patch of POPE lipid bilayer. The proteins are shown as ribbons colored by monomers and the lipids as licorices colored by atom names. Shown in the middle and bottom panels are the side views of the AQP4 model system. In the middle panel, waters are shown as dots and ions (Na and Cl) are all shown as spheres, all colored by atom names. In the bottom panel, proteins are shown as shadows and waters are shown as spheres colored by atom names. Colors by atom names: C, cyan; N, blue; H, white; O, red; Na, light yellow; Cl, green; S, yellow; P, red. The fully equilibrated system of AQP4 has the dimensions of $230\text{Å} \times 225\text{Å} \times 115\text{Å}$. It consists of 601596 atoms.

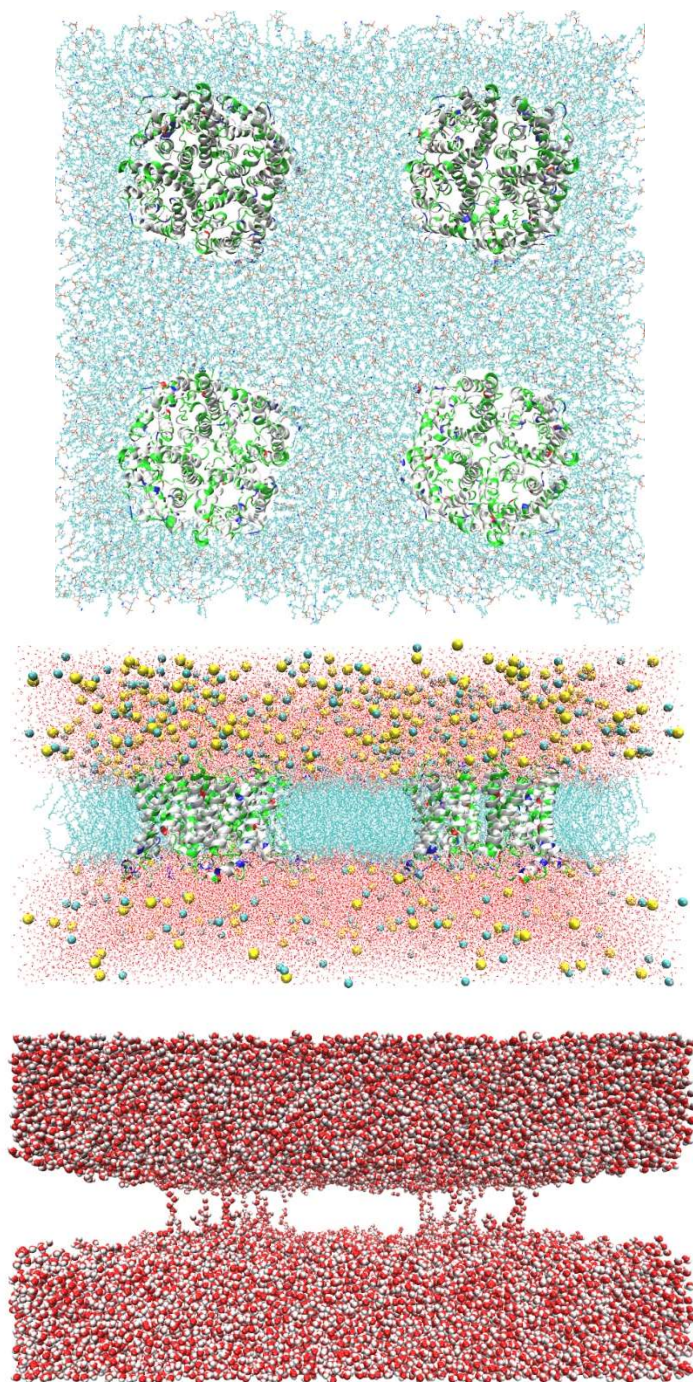


Fig. S2. Model system of AQP5 at 25°C. Shown in the top panel are the top view of four AQP5 tetramers (16 individual water channels/monomers) embedded in a patch of POPE lipid bilayer. The proteins are shown as ribbons colored by residue types and the lipids as licorices colored by atom names. Shown in the middle and bottom panels are the side views of the AQP5 model system. In the middle panel, waters are shown as dots and ions (Na and Cl) are all shown as spheres, all colored by atom names. In the bottom panel, waters are shown as spheres colored by atom names. Colors by atom names: C, cyan; N, blue; H, white; O, red; Na, light yellow; Cl, green; S, yellow; P, red. The fully equilibrated system of AQP5 has the dimensions of $224\text{Å} \times 224\text{Å} \times 114\text{Å}$. It consists of 569882 atoms.

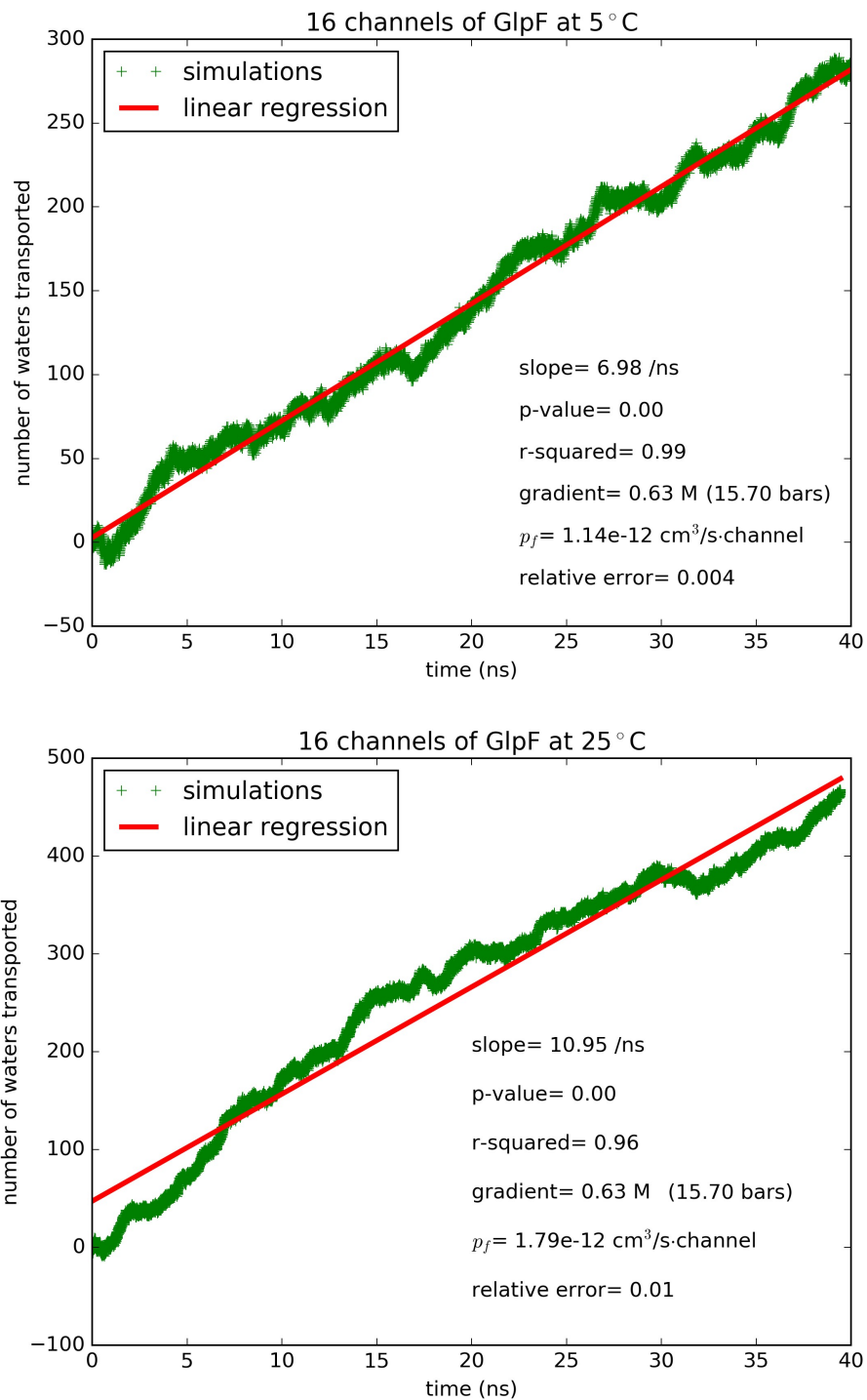


Fig.S3. Water flux through GlpF induced by osmotic gradient at two temperatures: (A) Top panel, 5°C. (B) Bottom panel, 25°C.

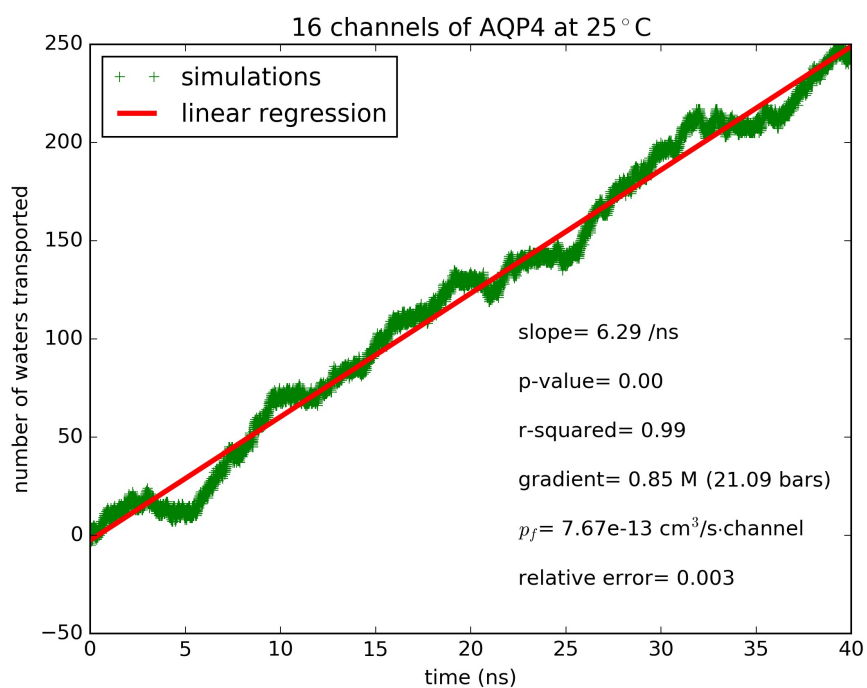
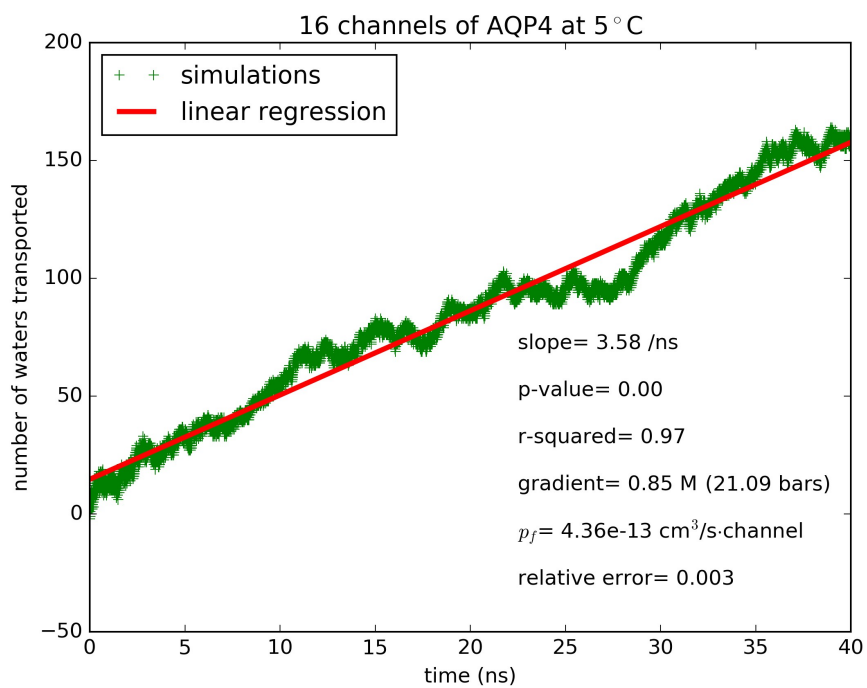


Fig. S4. Water flux through AQP4 induced by osmotic gradient at two temperatures: (A) Top panel, 5°C. (B) Bottom panel, 25°C.

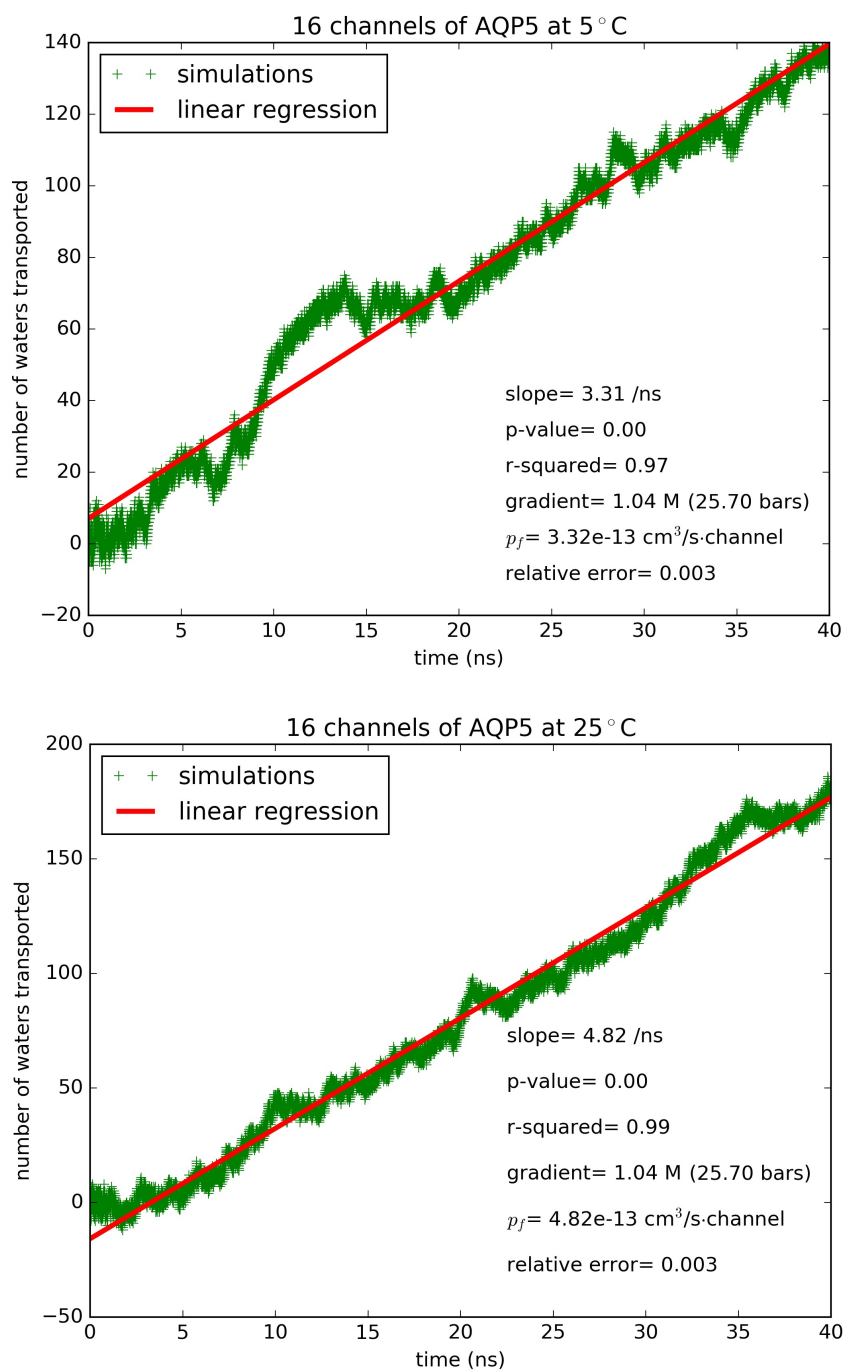


Fig. S5. Water flux through AQP5 induced by osmotic gradient at two temperatures: (A) Top panel, 5°C. (B) Bottom panel, 25°C.

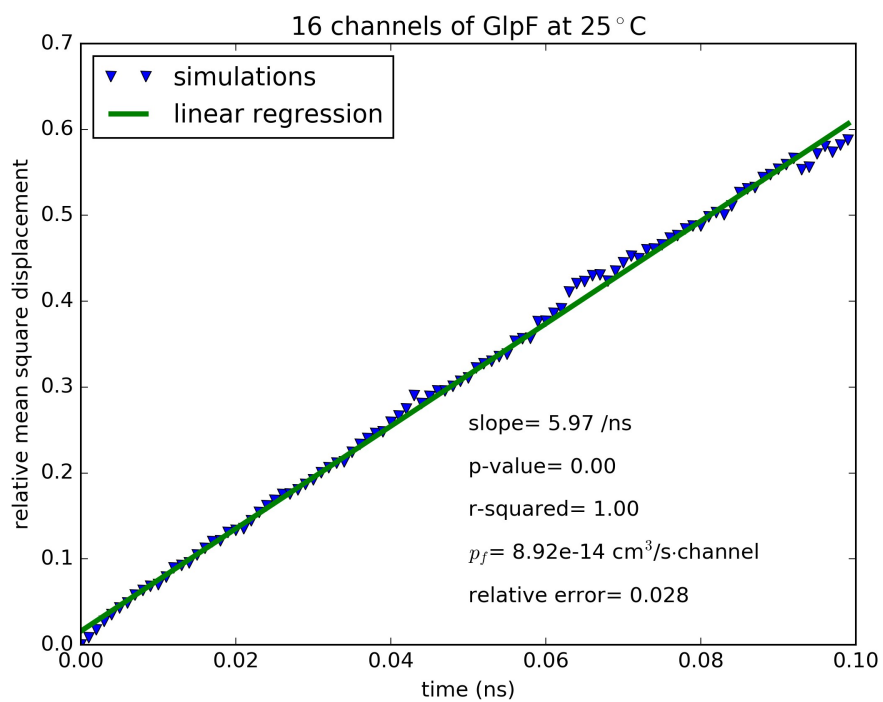
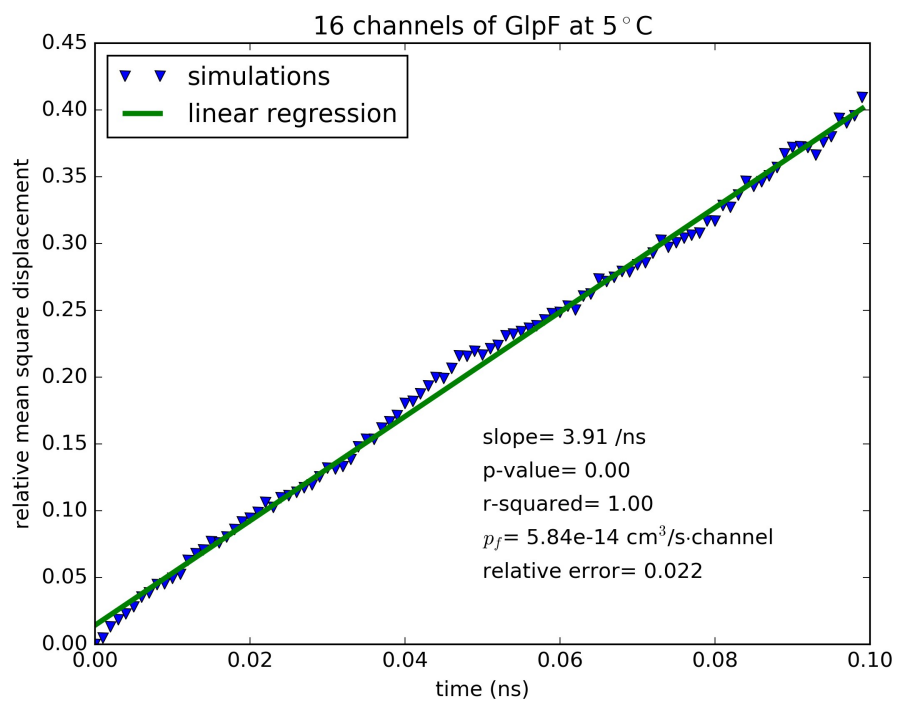


Fig. S6. Mean square displacement of waters inside the single-file region of the GlpF channel: (A) Top panel, 5°C. (B) Bottom panel, 25°C.

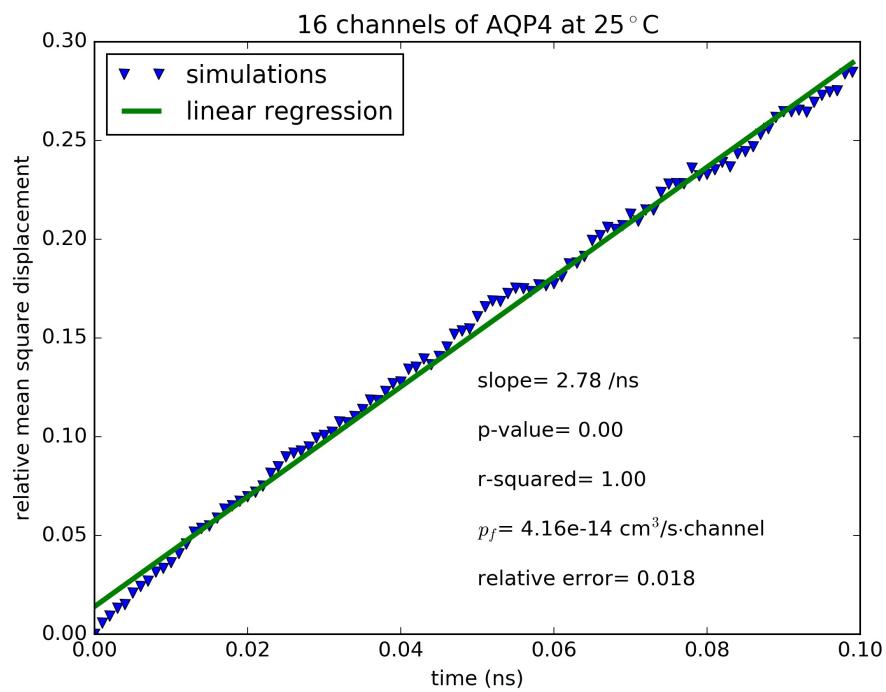
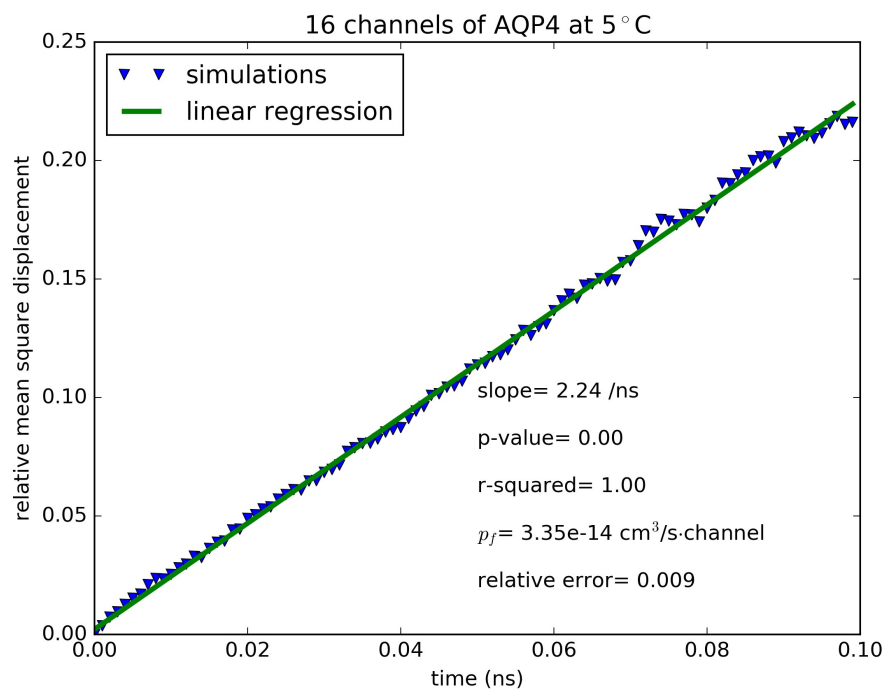


Fig. S7. Mean square displacement of waters inside the single-file region of the AQP4 channel: (A) Top panel, 5°C. (B) Bottom panel, 25°C.

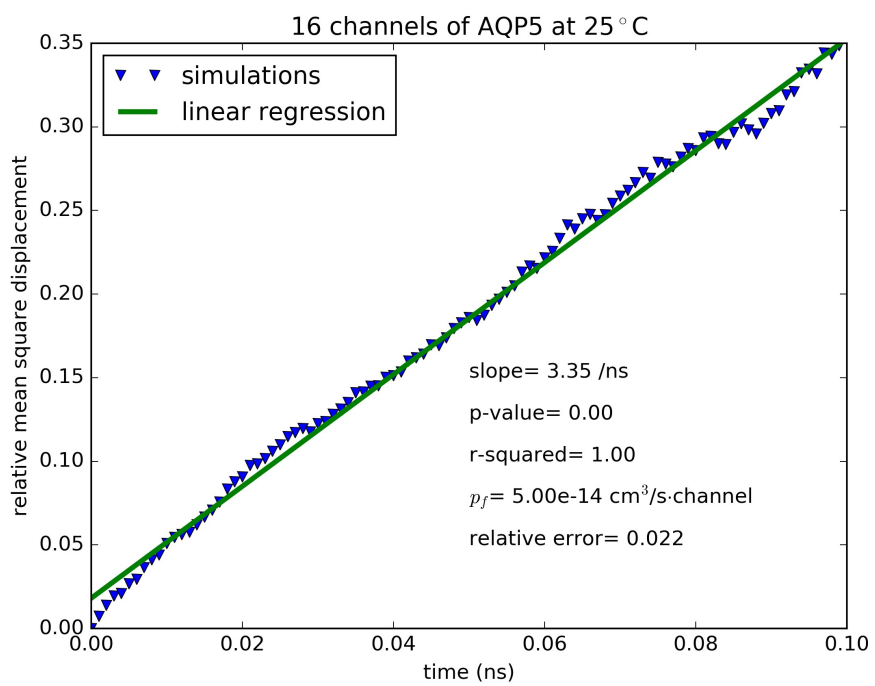
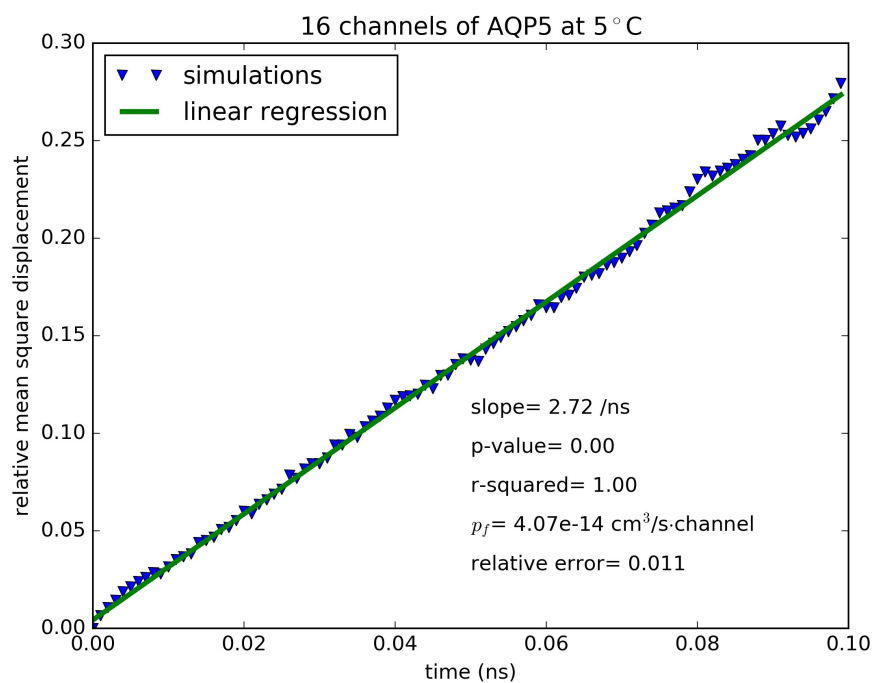


Fig. S8. Mean square displacement of waters inside the single-file region of the AQP5 channel: (A) Top panel, 5°C. (B) Bottom panel, 25°C.

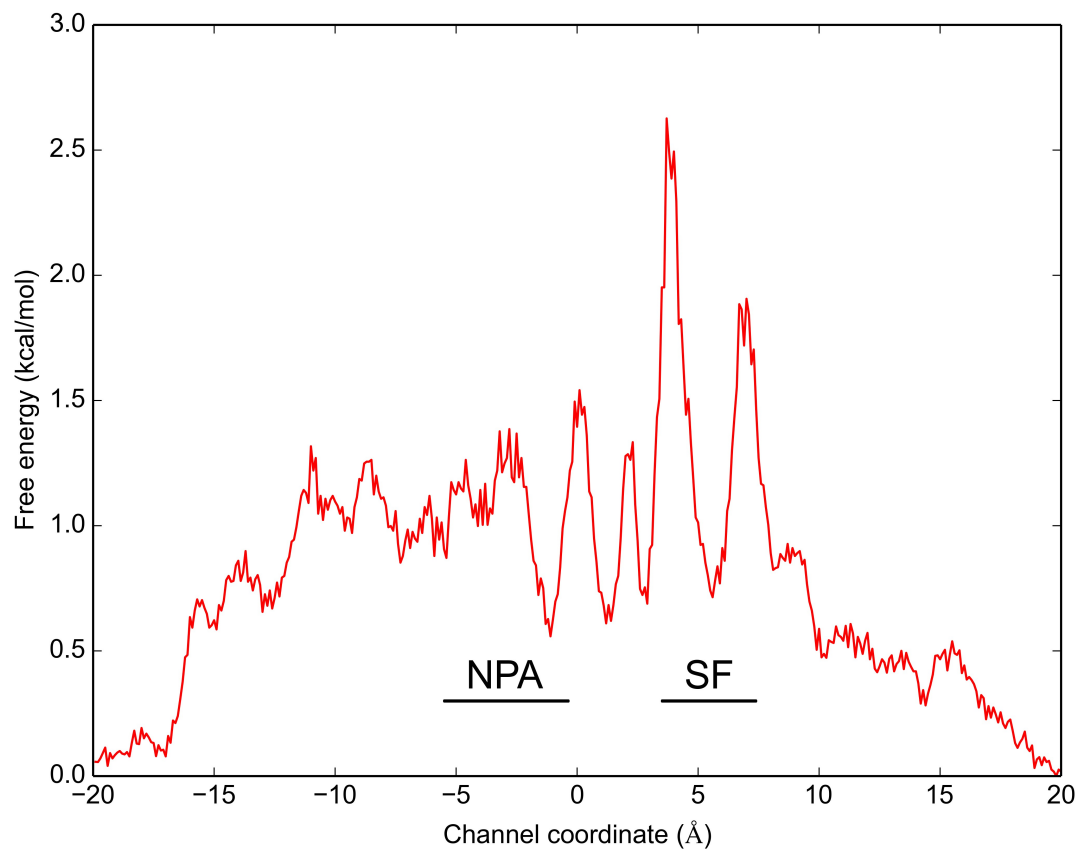


Fig. S9. Free energy profile of AQP4 for water permeation.

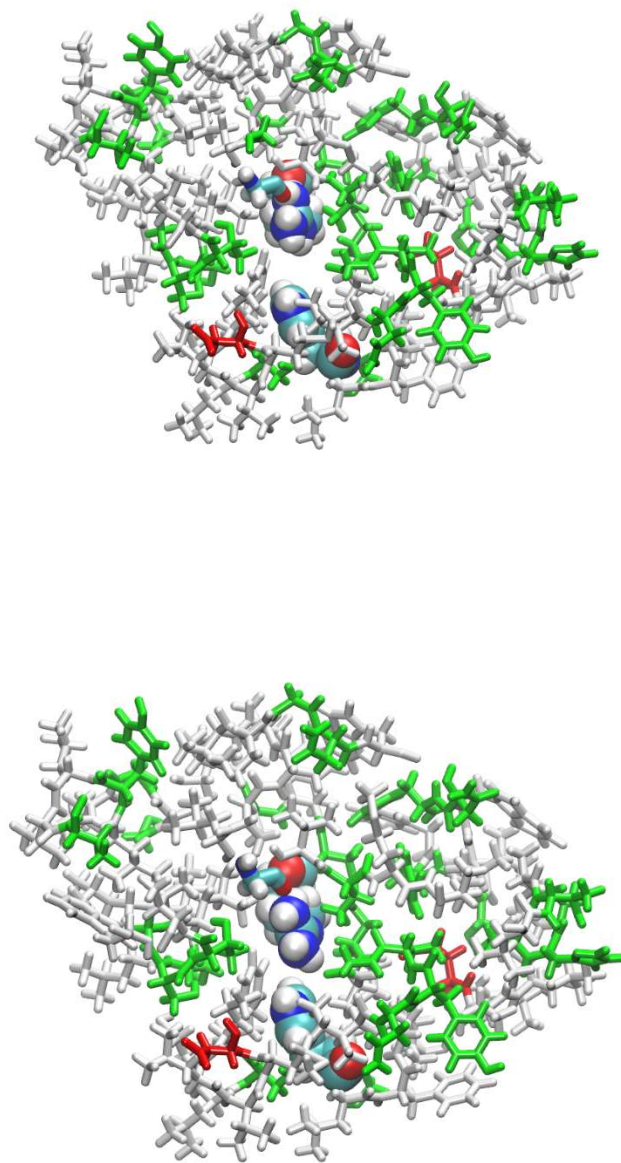


Fig. S10. AQP4 in the channel-open (top panel) and channel-closed (bottom panel) conformations. The ar/R selectivity filter forming residues Arg 216 and His 201 are shown as large spheres colored by atom names: C, cyan; H, white; O, red; N, blue. Other residues near the ar/R selectivity filter are shown as licorices colored by residue types: hydrophilic, green; hydrophobic, white; positive charged, blue; negatively charged, red. Gly 146 is shown as thick licorices colored by atom names. The carbonyl oxygens of Gly 146 and Arg 216 together anchor the sidechain of Arg 216.

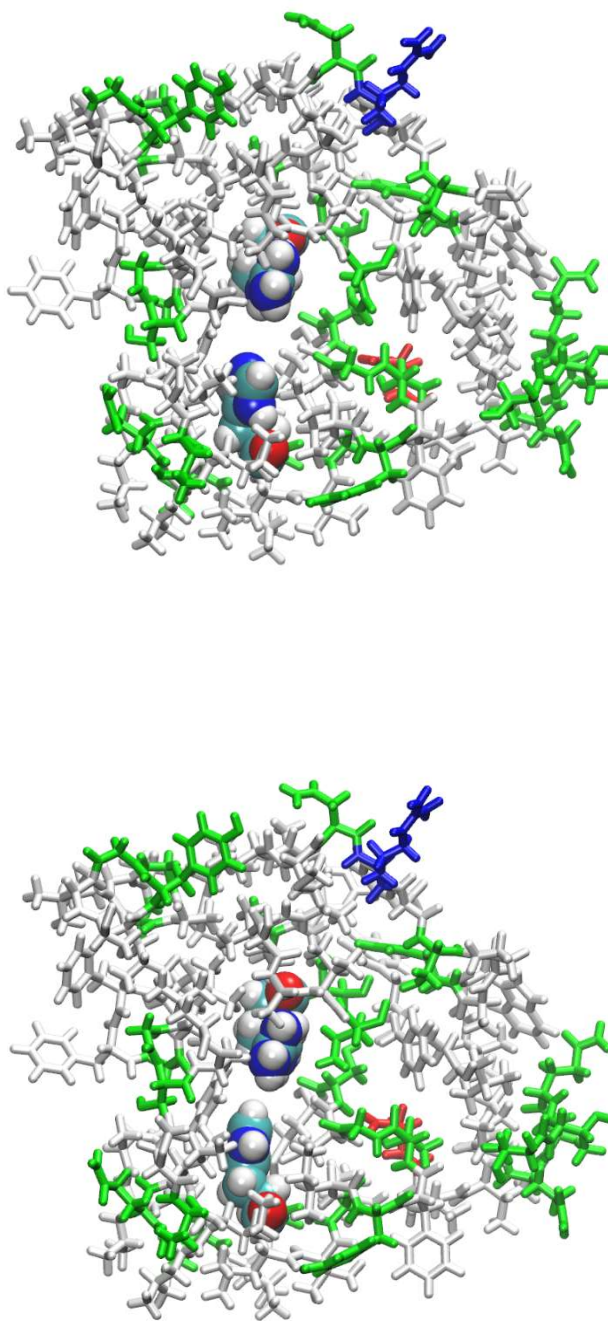


Fig. S11. AQP5 in the channel-open (top panel) and channel-closed (bottom panel) conformations. The ar/R selectivity filter forming residues Arg 188 and His 173 are shown as large spheres colored by atom names: C, cyan; H, white; O, red; N, blue. Other residues near the ar/R selectivity filter are shown as licorices colored by residue types: hydrophilic, green; hydrophobic, white; positive charged, blue; negatively charged, red.

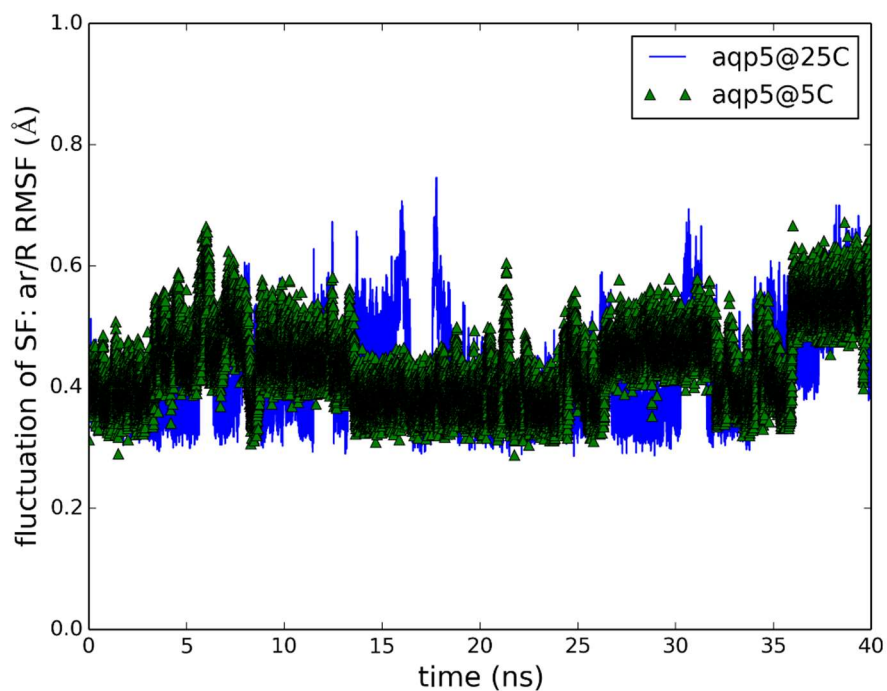
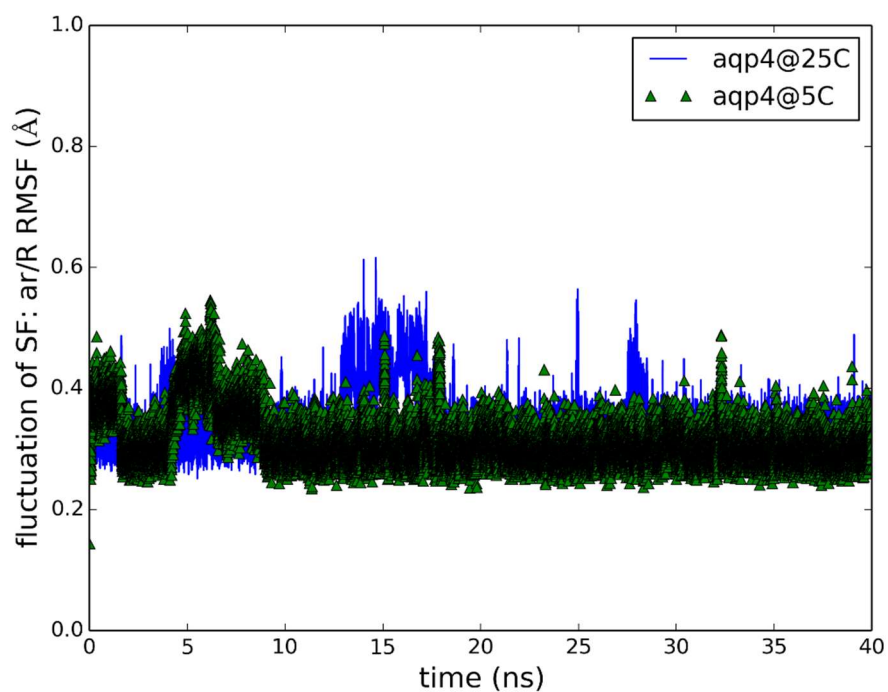


Fig. S12. Fluctuations of the ar/R selectivity filter of AQP4 and AQP5. Shown here are the root mean square deviations from the average structure of Arg 216 and His 201 of AQP4 (top panel) and the same for Arg 188 and His 173 of AQP5 (bottom panel).